Analytical and Bioanalytical Chemistry (2021) 413:1639–1649
https://doi.org/10.1007/s00216-020-03126-1

RESEARCH PAPER

"Turn-off" sensing probe based on fluorescent gold nanoclusters for the sensitive detection of hemin

Shemsu Ligani Fereja[1,2] · Zhongying Fang[1,2] · Ping Li[1,2] · Jinhan Guo[1,2] · Tadesse Haile Fereja[1,2] · Wei Chen[1,2]

Received: 28 October 2020 / Revised: 9 December 2020 / Accepted: 14 December 2020 / Published online: 23 January 2021

Abstract

Balanced level of hemin in the body is fundamentally important for normal human organ function. Therefore, environmentally benign, stable, and fluorescent metal nanoclusters (NCs) for selective and sensitive detection of hemin have been investigated and reported. Herein, highly orange red emissive gold NCs are successfully synthesized using glutathione as a reducing and stabilizing agent (GSH-Au NCs). The clusters are characterized using various techniques like Fourier transform infrared spectroscopy (FTIR), transmission electron microscopy (TEM), UV-vis spectroscopy, and fluorescence spectrometer. The fluorescence intensity of as-synthesized Au NCs strongly quenched upon addition of different concentrations of hemin. The decrease in fluorescence intensity of GSH-Au NCs has been applied for determination of hemin concentration in the linear range from 1 to 25 nM with a low limit of detection (LOD) of 0.43 nM. The method was also successfully applied for quantification of hemin in human serum sample. In view of this reality, the system can be considered as a possible strategy and excellent platform for determination of hemin in various areas of application.

Keywords Nanocluster · Turn-off · Emission · Fluorescence · Gold · Hemin

Introduction

Hemin is a natural porphyrinatoiron complex derived from processed red blood cells held in a heterocyclic ring [1, 2]. The electron transfer process of Fe (III)/Fe (II) reversible redox reaction in the body is enabled by hemin [3, 4]. Perhaps hemin plays a key role in normal human organ function by oxygen transportation [4, 5]. Moreover, in analytical applications, hemin is a substitute for natural enzymes [6]. It has also significant role during production of anticancer medicines [7]. In clinical applications, hemin is among the chief important iron supplements [8]. However, according to some scientific reports, availability of excess hemin in the body may interpolate in lipid membranes and enhance the catalytic process during radical formation [9]. Subsequently, death of the cell beside it can cause stroke and brain damage, as it is known that its deficiency enhances the production of carbon monoxide [2, 9, 10]. Numerous techniques have been reported in order to detect hemin and related substances, e.g., high performance liquid chromatography [11], spectrophotometric methods [12], voltammetric method [13], and chemiluminescence [3, 4]. However still, these techniques are time-consuming, complicated, not flexible to regular usage, and costly. Therefore, developing simple, robust, sensitive, and selective hemin detection methods is still paramount.

Currently, considerable attention is given to metal nanoclusters (MNCs). They are small in size (< 2 nm) and have adjustable energy level [14]. MNCs exhibit molecule-like optical and electronic characteristics [15, 16]. In particular, gold nanoclusters are special in their atom arranging structure and demonstrate distinct electronic structures and properties that are profoundly unlike metallic nanocrystals [17]. Commonly, they are ultra-small and protected by stabilizing agents with exhibiting intense fluorescence [18–21]. Recently, Au NCs were reported as fluorescent probe to quantify the level of different ions, biological molecules, and imaging purpose besides being used for catalysis [22]. This multipurpose application is because of their stable fluorescence, biocompatibility, fascinating performance, high colloidal

✉ Wei Chen
weichen@ciac.ac.cn

[1] State Key Laboratory of Electroanalytical Chemistry, Changchun Institute of Applied Chemistry, Chinese Academy of Sciences, Changchun 130022, Jilin, China

[2] University of Science and Technology of China, Hefei 230026, Anhui, China

stability, and superior catalytic activity [18, 23, 24]. Bian et al. have utilized glutathione-protected Au NCs (GSH-Au NCs) as fluorescent probe to detect Hg^{2+} and Pb^{2+} with LOD of 5 μM and 50 μM respectively [25]. The level of alkaline phosphatase in human osteosarcoma cells was detected using fluorescent gold nanoclusters by Deng and co-workers [26]. AkramYahia-Ammar et al. used fluorescent gold nanoclusters for drug delivery and imaging application [27]. Heng-Chia Chang and Ja-an Annie Ho have used gold nanoclusters for quantitative investigation of cholesterol and hydrogen peroxide level with LOD values of 0.8 μM and 1.4 μM, respectively [28]. As far as our knowledge is concerned, no report was made on using of glutathione-capped gold nanoclusters (GSH-Au NCs) for detection of hemin in human serum via both inner filter effect and hemin-artesunate-induced mechanisms.

In this study, we report an environmentally benign, one-pot, "green" gold nanocluster synthesis method, based on commercially available glutathione (GSH) as a stabilizing and reducing agent. The synthesis of Au NCs was performed at the temperature of 55 °C and the obtained clusters show strong orange red emission at $\lambda_{em} = 569$ nm. The developed method is capable of producing Au NCs with high stability, as well as low cost and strong fluorescence for highly selective and sensitive sensing application. We utilize the synthesized GSH-Au NCs for the detection of hemin via concentration-sensitive quenching of the fluorescence intensity. The detection mechanism is also proposed. Firstly, the fluorescence quenching is due to inner filter effect (IFE), and secondly, generated superoxide radicals $O_2^{\cdot-}$ from artesunate under the catalysis of hemin can oxidize the fluorescent GS-Au NCs, and subsequently lead to the fluorescence quenching.

Experimental section

Materials and chemicals

Artesunate, hemin, K_2CrO_4, NaCl,$CaCl_2$, $Ag(NO_3)$, $Zn(NO_3)_2{\cdot}6H_2O$, $Ni(NO_3)_2{\cdot}6H_2O$, $Co(NO_3)_2{\cdot}6H_2O$, KCl, $MgCl_2$, $HAuCl_4{\cdot}3H_2O$, and L-glutathione have been obtained from Aladdin Biochemical Technology Co., Ltd. (Shanghai, China). HCl, NaOH, D-glucose (Glu), fructose (Fru), sucrose (Suc), L-proline (Pro), bovine serum albumin (BSA), L-cysteine (Cys), L-lysine (Ly), glycine (Gly), DL-alanine (Ala), and urea have been purchased from Beijing Chemical Works (Beijing, China). Ultrapure Milli-Q water was used for all experimental activities.

Instrumentation

UV illuminator at 365 nm has been employed in order to take the dark-field images of Au NCs. The fluorescence studies have been performed using a RF-5301PC spectrofluorophotometer equipped with a Xenon lamp at emission spectral range of 400–700 nm (ex = 369 nm). Quartz cuvette with 1 cm path length has been used during fluorescence measurement. The excitation and emission slit width was 5 nm. The UV-vis spectrum for as-synthesized nanocluster has been measured using UV-3000 PC spectrophotometer. The particle size of the clusters was measured using transmission electron microscopy (TEM, JEM-2100F). Thermo Scientific™ Nicolet™ iS™ 50 FTIR Spectrometer was used to obtain FTIR spectra.

Synthesis of Au NCs

Preparation of glutathione-protected gold nanoclusters was realized by following published protocol [29] with some modification. Compared to the previous procedure, the amount of gold salt, reaction time, and reaction temperature has been optimized. With these optimization and modification, enhanced fluorescent intensity and properties are expected.

Finally, the optimized procedure in detail, 1 mL aqueous solution of gold salt ($HAuCl_4{\cdot}3H_2O$, 10 mM) has been added to glutathione solution (5 mL; 50 mM) through magnetic stirring at 800 rpm. Total volume of the solution was brought to 10 mL using 4 mL of pure water. The solution was heated at 55 °C under continuous stirring for 12 h. Gradually, the color of reaction mixture converted from colorless to light yellow. It has been considered as confirmatory test for formation of nanoclusters. After cooling down the solution to room temperature, GSH-Au NCs were precipitated in a water/ethanol (1:2) mixture solution via centrifugation at 8000 rpm for 30 min. Finally, the obtained Au NCs were dispersed in 5 mL of water and kept refrigerated until use. The concentration of the as-synthesized GSH-Au NCs was calculated from stock solution of gold salt based on previous literature [28] and estimated to be ~ 4.66 mM. It has been further diluted to different working solutions using buffer for fluorescence measurements.

Fluorescent detection of hemin

Phosphate buffer (pH 7.5) has been used for detection of hemin. For detection of hemin, artesunate (100 μL; 5 mM), hemin (20 μL with varies concentrations), and GSH-Au NCs (50 μL; 0.75 μM) were pipetted sequentially into 500 μL buffer solutions. The mixture was shaken thoroughly and further diluted to 1.0 mL using purified water. The fluorescent detection was conducted at room temperature with different incubation times. Firstly, the emission maxima was optimized with different excitation wavelengths for better fluorescence signal. The fluorescence spectra have been measured (ex = 369 nm; em = 569 nm).

Selectivity measurement

To investigate whether the developed method is selective for hemin, we evaluate the fluorescence response of Au NCs mixed with various cations (Zn^{2+}, Mg^{2+}, Ca^{2+}, K^{+}, Cr^{2+}, Na^{+}, Co^{2+}, Ni^{2+}, and Ag^{+}) and some biological-related species (D-glucose (Glu), fructose (Fru), sucrose (Suc), L-cysteine (Cys), L-lysine (Ly), glycine (Gly), DL-alanine (Ala), bovine serum albumin (BSA, 15 μg mL^{-1}), glutathione (GSH), L-proline (Pro), and urea). Twenty microliters of 30.0 μM and 20.0 μM of the abovementioned biological species and metal ion solutions was prepared, respectively, using phosphate buffer (pH 7.5) and mixed with an equal volume of Au NC solution with equivalent proportion. The fluorescence spectra were recorded after the reaction was incubated at ambient temperature.

Measurement of hemin in real sample

Purified serum sample 10-fold diluted using buffer was obtained from local hospital and directly used in the experiment. Well-established spiked method has been applied for hemin detection [30]. Firstly, about 300 μL aliquot of human serum was spiked with standard hemin with different concentrations (1–25 nM). Then, 100 μL of spiked solutions with various concentrations of hemin were mixed with 50 μL of 0.75 μM Au NC solution, and 400 μL of PBS buffer finally diluted to 1 mL with water and fluorescence measurement was performed after incubation for 5 min. The guidelines of Changchun Institute of Applied Chemistry have been followed for all experiment activities, and furthermore, it was approved by the research ethics committee.

Results and discussion

Synthesis and characterization of GSH-Au NCs

As presented in Scheme 1, in this work, environmentally benign synthesis of glutathione-protected GSH-Au NCs for fluorescence-based hemin detection from human serum is reported. The gold salt ($HAuCl_4$) and glutathione (GSH) solution were mixed using magnetic stirrer at 800 rpm followed by heating at 55 °C under continuous stirring for 12 h. Throughout the reaction, the color of the solution has been converted from colorless to light yellow; this is considered as a conformation for gold nanocluster formation [31]. The vigorous stirring with heat treatment can lead to the reduction of Au^{3+} to Au^{0} and here GSH serves as both stabilizing and reducing agent. The as-synthesized Au NCs in this work have the following advantages in comparison to those reported previously [18, 32–35]: Utilization of low concentration of gold salt, high stability at room temperature, simple and green approach followed to prepare Au NCs in water without using any hazardous agents or solvents, no utilization of harsh reducing agent. All these experimental conditions exclude the chance of toxicity to the biological systems. Such one-pot reaction makes the synthesis procedure eco-friendly and simple as well as in agreement with the current green chemistry concept. Finally, the synthesized Au NCs exhibit strong fluorescent signal with an emission maximum of 569 nm.

Surface plasmon resonance (SPR) absorption commonly observed at visible region (500–550 nm) is a typical characteristic of AuNPs, while small Au NCs have no SPR peaks [36, 37]. Accordingly, the UV-vis absorption spectrum of as-synthesized Au NCs in this work was first measured to examine the absorption features. As illustrated in Fig. 1a, the UV-vis absorption spectrum of as-prepared Au NCs exhibits neither surface plasma resonance absorption peak nor molecular-like absorption in the mentioned regions, which indicates that small-sized (< 3 nm) Au NCs have been successfully prepared [23, 38, 39]. As illustrated in Fig. 1b, the as-prepared Au NCs show strong fluorescent intensity at 569 nm under excitation wavelength of 369 nm. Meanwhile, as compared in Fig. 1a insets, the solution has a light yellow color under sun light but shows orange red color under UV lamp irradiation (365 nm). These fluorescence measurements indicate again the small core size of the prepared GSH-protected Au clusters [31]. Besides the small size of the cluster, the fluorescence signals for gold nanoparticles are highly depending on the surface

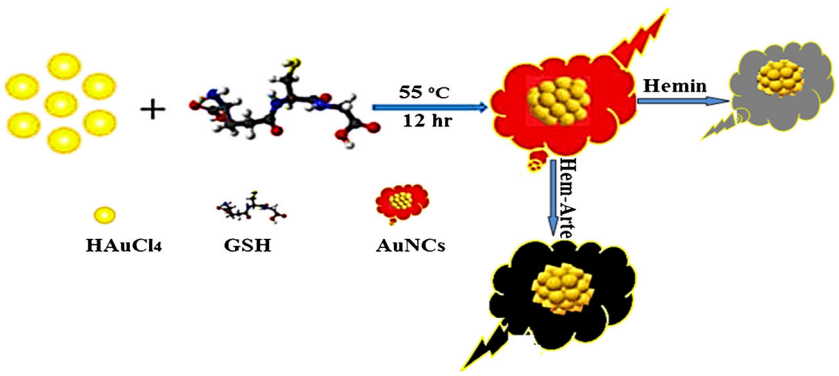

Scheme 1 Schematic representation of overall synthesis of Au NCs and fluorescent hemin detection

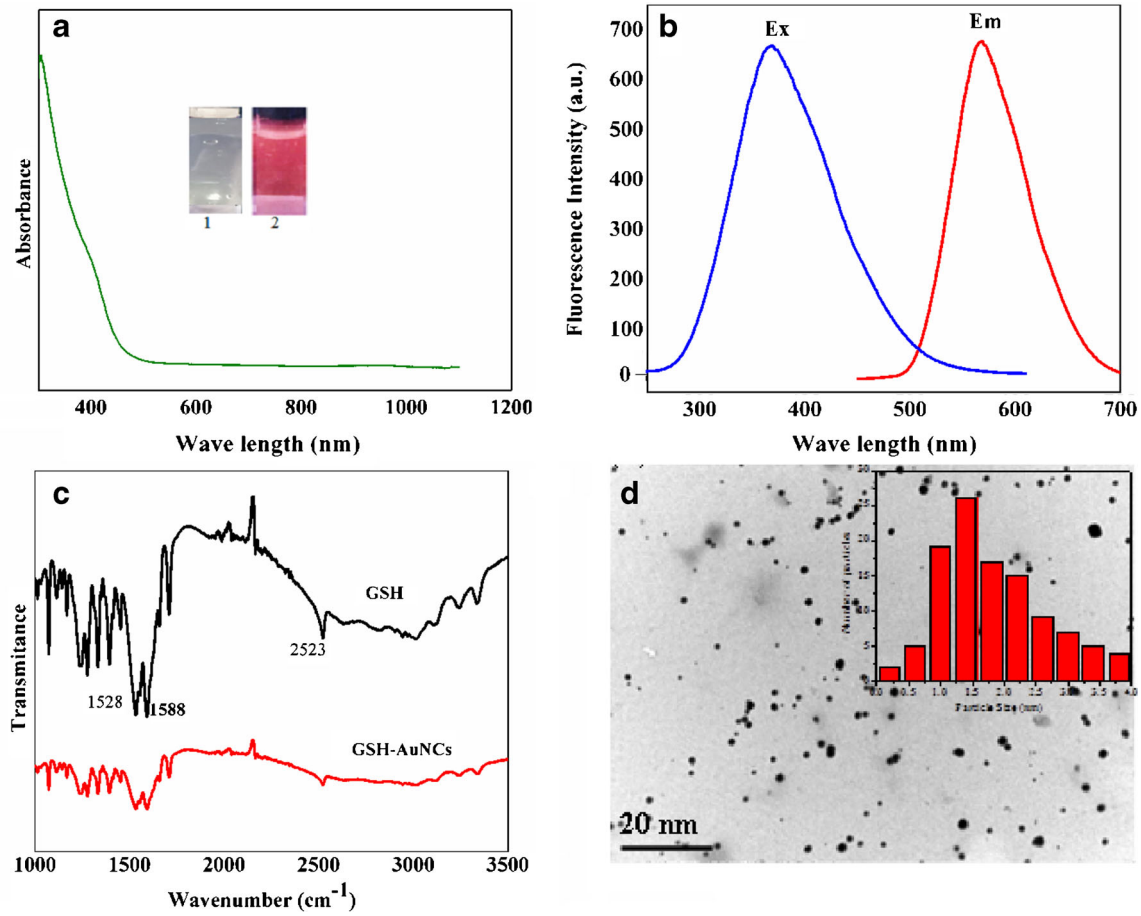

Fig. 1 **a** UV-vis absorption spectrum of the prepared GSH-Au NCs; the insets are the photographs of Au NC solution under room light (1) and UV lamp at 365 nm (2). **b** Excitation and emission spectra of the GSH-Au NCs (λ_{ex} = 369 nm, λ_{em} = 569 nm). **c** Fourier transform infrared (FTIR) spectra of GSH (black curve) and GSH-Au NCs (red curve). **d** TEM image of the GSH-Au NCs, and inset shows the cluster size distribution

ligands (-SR). Literature reports revealed that the fluorescence signal is affected by two different mechanisms: (i) through ligand to metal particle core charge transfer (LMNCT) via Au-S bond, and (ii) via donated delocalized electrons to the metal core from electron-rich atoms/groups of ligand [27, 40–42]. On the other hand, FTIR measurements were also

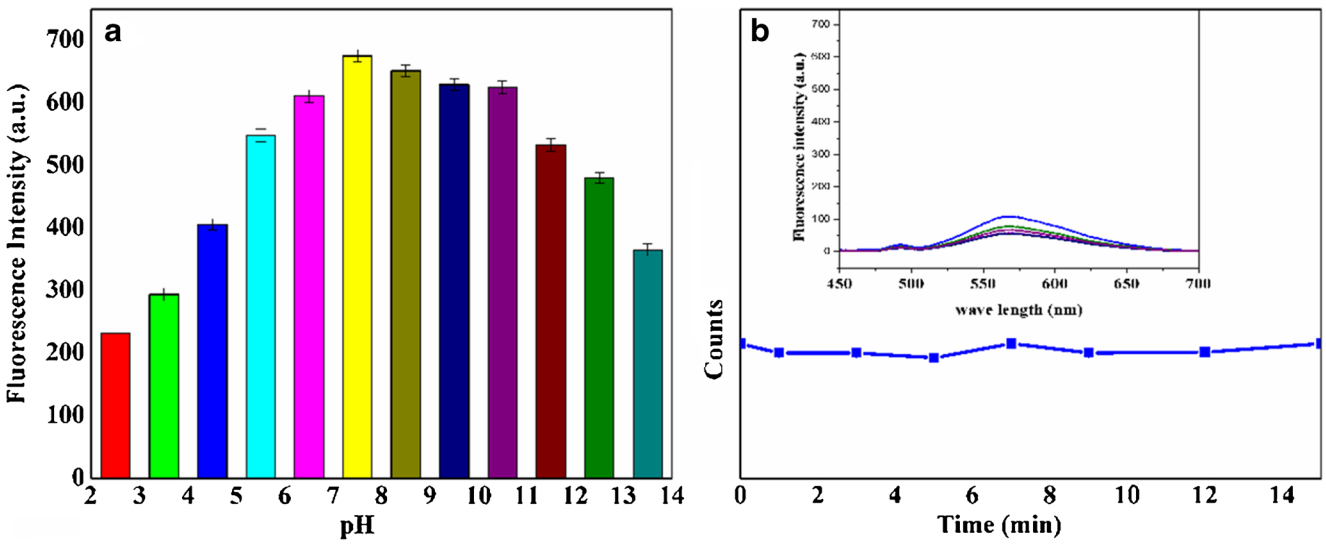

Fig. 2 **a** Fluorescence response of Au NCs toward different pH values. **b** Fluorescence response of Au NCs with various incubation times

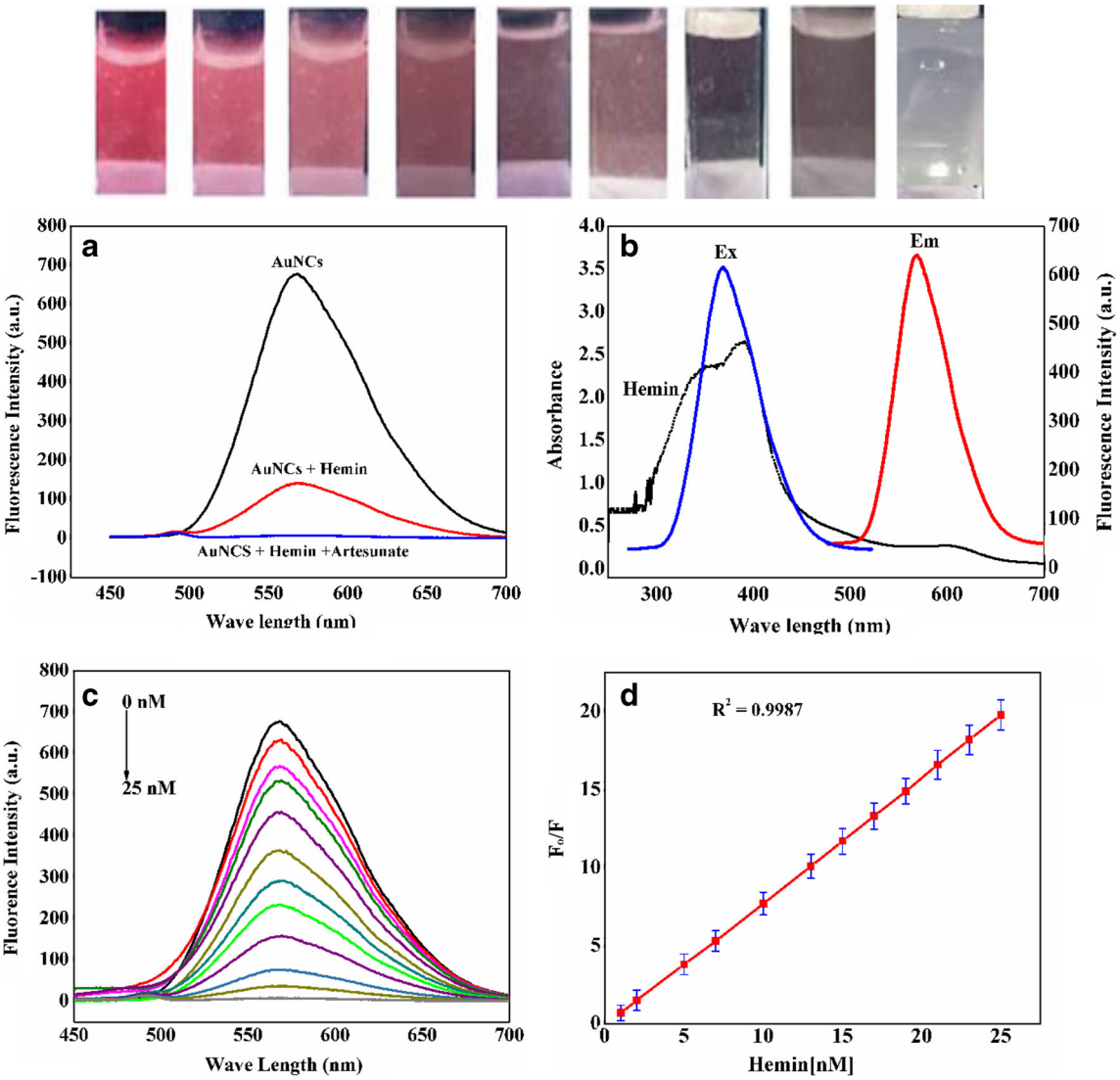

Fig. 3 **a** Fluorescent emission spectra of Au NCs in the absence (black curve), presence (red curve) 25 nM of hemin and the presence of 25 nM hemin-artesunate solution (blue curve). **b** Emission and excitation spectra of the Au NCs overlapped with UV-vis absorption band of the hemin. **c** Fluorescence spectra of Au NCs upon introduction of various concentrations of hemin. The concentration of artesunate is 5 mM. **d** The dependence of fluorescence response (F_0/F) on the concentration of hemin from 1 to 25 nM. Furthermore, it confirms the linear relationship between the F_0/F value and the concentration of hemin within a given range from 1 to 25 nM. The color of the solution under UV lamp upon the addition of different concentrations of hemin is also shown

carried out in order to study the influence of the ligands and to figure out the surface change of Au NCs. As presented in Fig. 1c, compared to pure GSH, the S-H stretching band at 2523 cm^{-1} is significantly reduced for the GSH-Au NCs, confirming the covalent bond formation between GSH thiols and Au NCs (the observed low absorption may be from the GSH weakly absorbed on the Au cluster surface) [43]. Moreover, the FTIR absorption peaks at 1528 and 1588 cm^{-1} from the GSH-Au NCs can still be observed, indicating the GSH ligand capping on the cluster surface [44].

To directly observe the core size of the prepared Au NCs, TEM measurement was then performed. As shown in Fig. 1d, the TEM image reveals that all produced clusters are well distributed having a size range of 1–4 nm. All above optical and TEM characterizations indicate clearly that ultra-small Au nanoclusters with unique fluorescence have been successfully produced under the protection of GSH ligands [44, 45].

Fluorescence properties of the synthesized GSH-Au NCs

From above results, as-prepared GSH-Au NCs exhibit strong fluorescence. The effects of different environmental factors on the fluorescence are therefore investigated. In order to examine the impact of pH on the fluorescence response, Au NCs have been dispersed in 0.1 M PBS and the desired value of pH was adjusted using 0.1 M NaOH or HCl. As illustrated in Fig. 2a, reduced fluorescence intensity of Au NCs has been

Scheme 2 The proposed fluorescence quenching mechanism of Au NCs by hemin-artesunate solution

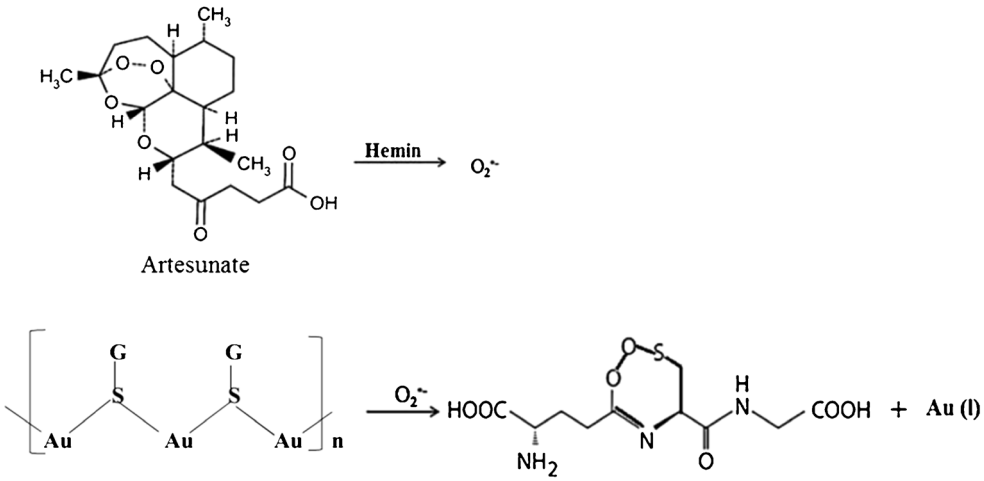

observed in high acidic medium. This may be due to the destabilization of GSH-protected gold nanoclusters due to electron transfer from Au NCs to the medium [30]. In contrast, the fluorescence intensity is not quenched significantly in basic media. Even though the prepared GSH-Au NCs are stable within the pH range of 5–12, neutral pH (pH = 7.5) is preferred as the optimal condition. In fact, the highest fluorescence intensity was obtained at this pH condition, as seen from Fig. 2a.

Fluorescence impacts of ionic strength have been evaluated using NaCl salt. Fluorescence measurement was made after introduction of various concentrations of NaCl solution into the Au cluster solution. However, no significant change in fluorescence response was observed upon an increment of NaCl concentration. Based on such result, the fluorescence intensity of Au NCs is not influenced by ionic strength under a given experimental condition. This shows that high stability of the GSH-protected gold nanocluster and no aggregation of nanocluster occurred under the high-salt condition [46]. The room temperature stability of the nanocluster at various time intervals is explored. It has been observed that the Au NCs are highly stable at room temperature for more than 1400 min without decrease of the original fluorescence intensity. The obtained experimental results revealed that the synthesized gold nanocluster can be applied for a type of excellent fluorescence-sensing probe at optimal conditions for the detection of hemin. Before the detection procedure is performed, the impacts of incubation time between hemin-artesunate mixture and GSH-Au NCs were investigated. The mixture was shaken sufficiently and the fluorescence intensity was recorded within different time intervals. Even though there is no significant difference, 5-min incubation period is the most suitable for detection of hemin, as shown in Fig. 2b.

Fluorescence detection of hemin by GSH-Au NCs

Highly fluorescent glutathione-capped gold nanocluster for detection of hemin was developed. In the absence of hemin, the synthesized nanoclusters exhibit strong fluorescent signal with an emission and excitation maximum of 569 and 369 nm respectively (Fig. 1b). However, the fluorescence intensity of the cluster is highly quenched after 25 nM hemin was added. Interestingly, the cluster solution also shows almost no fluorescent signal upon introduction of about 25 nM hemin-artesunate solution, as observed from Fig. 3 a. Furthermore, the addition of artesunate without hemin has negligible effect

Table 1 Detection performances (LOD) of fluorescence methods based on different materials for detection of hemin

	Sample type to be applied	Main interferents	Material	Technique	LOD	Reference
1	Water and blood	Cations and biomolecules	Cytidine-Cu NCs	Fluorescence	0.045 μM	[47]
2	Serum	Cations and biomolecules	Artemisinin-thiamine	Fluorescence	0.68 nM	[2]
3	Beef	Cations and biomolecules	Graphene transistor	Fluorescence	10 nM	[50]
4	Human blood	Cations and biomolecules	Graphitic carbon nitride nanosheets	Fluorescence	0.15 μM.	[51]
5	_	Biomolecules	A label-free DNA reduced graphene oxide	Fluorescence	50 nM	[52]
6	Serum	Cations and biomolecules	Nitrogen–sulfur co-doped carbon dots (CDs)	Fluorescence	0.1 μM.	[53]
7	_	Cations	Capped carbon dots (CDs/β-cd)	Fluorescence	1 μM	[54]
8	_	Biomolecules	Protoporphyrin IX binding to G-quadruplexes	Fluorescence	36 nM	[10]
9	Serum	Cations and biomolecules	GSH-Au NCs	Fluorescence	0.43 nM	Present work

Table 2 Comparison of the present method with previously reported methods for the detection of hemin

	Technique	Linear range	LOD	Reference
1	Differential pulse voltammetry	1.0×10^{-19}–1.0×10^{-6} M	7.5×10^{-20} M	[55]
2	Voltammetric method	0.020–2.60 μM	3.16×10^{-3} μM	[5]
3	Chemiluminescence	8.6×10^{-10}–8.6×10^{-7}M	8.6×10^{-11}M	[8]
4	Chemiluminescence	1.0–100.0 nM	0.37 nM	[3]
5	Spectroscopic method	1–250 μM	91 nM	[56]
6	Fluorescence	1–25 nM	0.43 nM	Present work

on the fluorescence response of the synthesized nanocluster. Based on these facts, a possible mechanism has been proposed.

As illustrated in Fig. 3b, the Au NCs show excitation band at 369 nm and emission bands at 569 nm. On the other hand, hemin shows broad absorptions at 263, 348, 388, and 591 nm, indicating several overlaps between the excitation and emission bands of gold nanoclusters and the absorption bands of hemin. This spectral overlapping indicates that the fluorescence quenching after addition of hemin is most probably due to inner filter effects of hemin on the fluorescence of Au NCs [47, 48].

Furthermore, it has been well studied that hemin has the ability to catalyze the decomposition of artesunate by producing superoxide radicals of $O_2^{\bullet-}$, as demonstrated in Scheme 2 [3, 4, 6, 7]. At the same time, recently investigated work revealed that the fluorescence of Au NCs can be easily quenched by oxygen at exited states, Au NC* + $^3O_2$ → Au NC + $^1O^*_2$ [30, 38]. Therefore, the fluorescent GSH-Au NCs are easily oxidized to non-fluorescent solution due to the generated superoxide radicals and the Au NCs probably change their oxidation state from 0 to I or III, resulting in the fluorescence quenching dependent on the concentration of added hemin. Therefore, the total fluorescence quenching could be attributed cumulatively from inner filter effect and oxidation of gold by in situ-generated superoxide radicals (Scheme 2).

Figure 3c illustrates the fluorescence spectra of GSH-Au NCs up on addition of hemin-artesunate solution with various concentration range (1 to 25.0 nM). Before the spiking procedure was performed, the unspiked samples have been checked for the presence of hemin and no traces of hemin were detected in purified serum sample. It can be seen that the fluorescence intensity of the GSH-Au NCs gradually decreases with increasing the amount of hemin-artesunate solution from 1 to 25 nM. Especially, with the presence of 25 nM hemin-artesunate, the fluorescence intensity of GSH-Au NCs is almost completely quenched. Correspondingly, the GSHs-Au NC solution color under UV lamp shows gradual change with the presence of different concentrations of hemin-artesunate and almost no color can be observed finally after the addition of 25 nM hemin-artesunate (Fig. 3c). As shown in Fig. 3d, the F_o/F displays a good linear relationship with hemin concentration ranged from 1 to 25.0 nM ($R^2 = 0.9987$). Meanwhile,

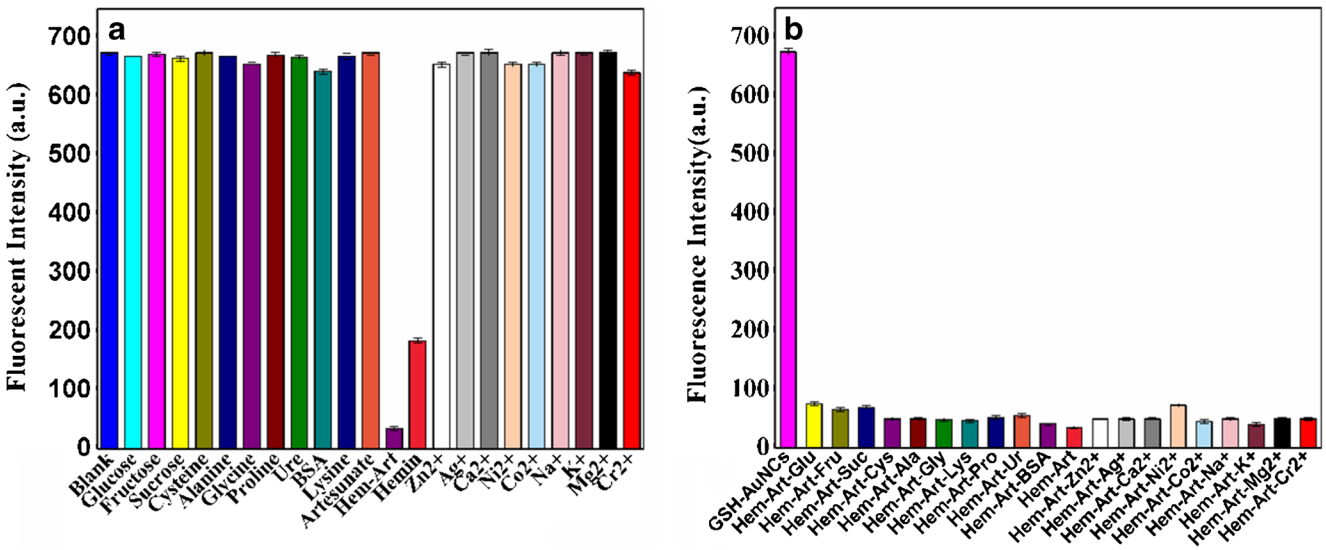

Fig. 4 **a** Fluorescence intensity of Au NCs after addition of hemin and hemin-artesunate mixture and various interfering substances separately. The concentration of all interfering substances is 0.5 mM. **b** Fluorescence intensity of Au NCs after introduction of hemin-artesunate mixture and other interfering substances

Table 3 Recoveries of hemin spiked in serum ($n = 5$)

Sample	Spiked (nM)	Found ± S.D.	% Recovery	RSD (%)
Serum	1	1.07±0.051	107	4.67
	1.5	1.4±0.042	93.33	3.00
	3	2.96±0.15	98.66	5.06
	4	3.91±0.061	97.75	1.56
	5	5.08±0.091	101.6	1.79
	5.5	5.7±0. 177	103.63	3.10
	7	7.03±0.167	100.4	2.38
	8	8.05±0.282	100.6	3.5
	9	8.81±0.423	97.88	4.80
	9.5	9.33±0.476	98.2	5.10
	11	11.02±0.711	100.1	6.45
	12	12.03±0.667	100.2	5.54
	13	12.91±0.795	99.3	6.15
	14	13.94±0.858	99.5	6.12
	15	15.03±0.823	100.2	5.47

the calculated limit of detection (LOD) was found to be 0.43 nM at a signal-to-noise ratio of 3, which is much lower than the maximum level (10 μM) of hemin in human body [49]. These outcomes verify as-synthesized Au NCs can be used as sensitive probes for the fluorescence detection of hemin.

Table 1 illustrates the detection performance of the present method in comparison with previously reported fluorescent methods with different materials. Accordingly, the LOD of hemin by this method is much lower than those of the previously reported fluorescence methods or sensing systems. On the other hand, the developed detection system has been compared with other detection techniques in terms of LOD and linear range, as displayed in Table 2. The present method shows better sensitivity than others and the linear range is also comparable with the reported detection techniques. The repeatability and reproducibility of the present method were also investigated and the relative standard deviations (RSD) are 2.7% and 6.5%, respectively, confirming the high reliability of the present proposed method.

Cations and biological molecules are naturally found in the human body particularly in the serum. Moreover, they are known as potential interferences for hemin and some of the biological molecules are known as chelating ligands to possibly form complexes with gold and thus affect the fluorescence response. Therefore, the selectivity performance of the developed method for hemin detection has also been examined by measuring the intensity change of gold nanoclusters in the presence of various common cations (Zn^{2+}, Mg^{2+}, Ca^{2+}, K^{+}, Cr^{2+}, Na^{+}, Co^{2+}, Ni^{2+}, and Ag^{+}) and biomolecules (D-glucose, (Glu), fructose (Fru), sucrose (Suc), L-proline (Pro), bovine serum albumin (BSA), urea, L-cysteine (Cys), L-lysine (Ly), glycine (Gly), and DL-alanine (Ala)). From the fluorescence intensity change and the corresponding fluorescence spectra illustrated in Fig. 4a, the fluorescence intensity of the Au NCs obviously decreases after introduction of hemin and hemin-artesunate mixture. On the other hand, the fluorescence responses of Au NC solution mixed with other interfering substances and blank (GSH-Au NCs) solution are almost the same. Furthermore, the fluorescence quenching capacity of the mixture of hemin-artesunate and the interfering metal ions and biomolecules were also investigated. The same fluorescence response was observed before and after the introduction of these possible interfering substances, as demonstrated by Fig. 4b. These results clearly indicate that the present detection strategy using glutathione-capped Au NCs is profoundly selective and sensitive toward detection of hemin.

Through oxidative and non-oxidative mechanism, excess availability of hemin in the human body fluid can be potentially toxic and normal level of hemin in biological fluid should be 3–10 μM [49]. To examine the practical application of the as-synthesized Au NCs for hemin detection, numerous concentrations of hemin ranged from 1 to 15 nM were spiked into a diluted human serum sample. Blank serum sample has been evaluated for its fluorescence response before spiking procedure. The result indicates that no obvious response to

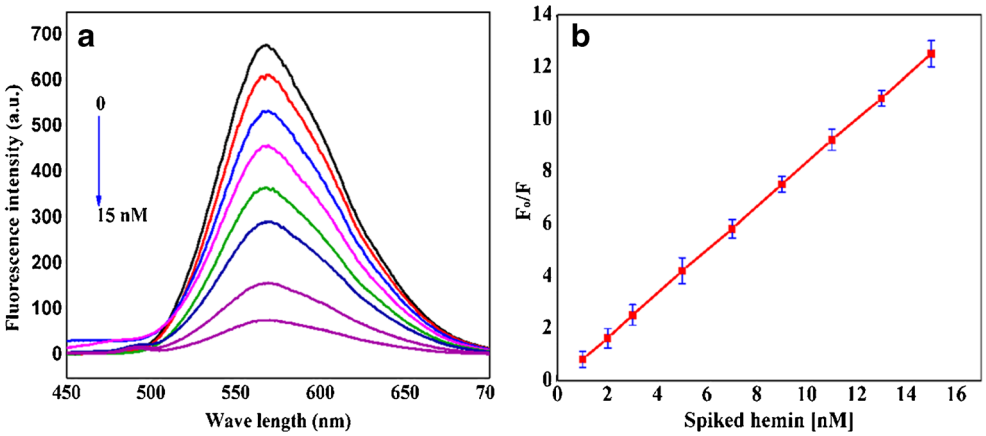

Fig. 5 **a** Fluorescence spectra of Au NCs in the real serum sample spiked with various concentrations of hemin (1–15 nM) and **b** the corresponding fluorescence intensity versus concentration of spiked hemin

the blank sample was observed. This result signifies that serum sample has no obvious effect on the performance of the method.

Figure 5a shows the fluorescence spectra of the GSH-Au NCs in hemin-spiked serum sample. As well illustrated in Fig. 5a, after the nanocluster solution was spiked with various concentrations of hemin, the fluorescence intensity gradually decreased. Moreover, from Fig. 5b, the plot of F_0/F versus different concentration of hemin-spiked serum shows linear relationship in the range of 1 to 15 nM, with R^2 value of 0.9957. The calculated detection limit was as low as 0.720 nM. Table 3 illustrates the recovery study result of hemin-spiked serum sample. Obviously, the high recoveries indicate the satisfied practicality of the GSH-Au NC fluorescence probes for real sample determination. Based on these facts, it can be concluded that the developed Au NC-based fluorescence system is highly attractive for practical determination of hemin in the biological body fluids in general and in the human serum specifically.

Conclusions

In this work, we synthesized glutathione-stabilized fluorescent gold nanoclusters for rapid, selective, and sensitive detection of hemin in human serum. Based on the investigations made, the resulting Au NCs demonstrate strong red fluorescence and good stability at room temperature. The detection mechanisms of as-prepared Au NCs were also investigated. Among the advantages of the present gold cluster-based method, it is environmentally friendly, highly stable, highly sensitive, and selective than most of the reported sensing methods for hemin determination. Therefore, the approach we followed could probably be used as a good platform for the developments of less costly, sensitive, and environmentally friendly bio probe for hemin detection.

Funding This work was funded by the National Natural Science Foundation of China (Nos. 21575134, 21633008, 21773224), National Key Research and Development Plan (2016YFA0203200), K. C. Wong Education Foundation, Natural Science Foundation of Guangxi Province (2019GXNSFGA245003), and Chinese Government Scholarship under China Scholarships council (CSC).

Compliance with ethical standards

Conflict of interest The authors declare that they have no conflict of interest.

References

1. Lee JM, Lee WH, Kay HY, E-s K, Moon A, Kim SG. Hemin, an iron-binding porphyrin, inhibits HIF-1α induction through its binding with heat shock protein 90. Int J Cancer. 2012;130:716–27. https://doi.org/10.1002/ijc.26075.
2. Ni P, Chen C, Jiang Y, Lu Y, Chen W. A simple and sensitive fluorescent assay for hemin detection based on artemisinin-thiamine. Sensor Actuat B: Chem. 2018;273:198–203. https://doi.org/10.1016/j.snb.2018.06.052.
3. Gao W, Wang C, Muzyka K, Kitte SA, Li J, Zhang W, et al. Artemisinin-luminol chemiluminescence for forensic bloodstain detection using a smart phone as a detector. Anal Chem. 2017;89:6160–5. https://doi.org/10.1021/acs.analchem.7b01000.
4. Fereja TH, Kitte SA, Gao W, Yuan F, Snizhko D, Qi L, et al. Artesunate-luminol chemiluminescence system for the detection of hemin. Talanta. 2019;204:379–85. https://doi.org/10.1016/j.talanta.2019.06.007.
5. Jahromi Z, Shamspur T, Mostafavi A, Mohamadi M. Separation and preconcentration of hemin from serum samples followed by voltammetric determination. J Mol Liq. 2017;242:91–7. https://doi.org/10.1016/j.molliq.2017.07.008.
6. Han J, Zhou Z, Bu X, Zhu S, Zhang H, Sun H, et al. Employing aqueous CdTe quantum dots with diversified surface functionalities to discriminate between heme (Fe(ii)) and hemin (Fe(iii)). Analyst. 2013;138:3402–8. https://doi.org/10.1039/C3AN00310H.
7. Ikariyama Y, Suzuki S, Aizawa M. Luminescence immunoassay of human serum albumin with hemin as labeling catalyst. Anal Chem. 1982;54:1126–9. https://doi.org/10.1021/ac00244a026.
8. Han S, Liu E, Li H. Flow injection chemiluminescence determination of hemin using the rhodamine B–H_2O_2–NaOH system. Microchim Acta. 2005;149:281–6. https://doi.org/10.1007/s00604-004-0312-5.
9. Sawicki KT, Chang H-C, Ardehali H. Role of heme in cardiovascular physiology and disease. J Am Heart Assoc. 2015;4:e001138–e. https://doi.org/10.1161/JAHA.114.001138.
10. Kang BH, Li N, Liu SG, Li NB, Luo HQ. A label-free, highly sensitive and selective detection of hemin based on the competition between hemin and protoporphyrin IX binding to G-quadruplexes. Anal Sci. 2016;32:887–92. https://doi.org/10.2116/analsci.32.887.
11. Rong X-J, Tang M-Q, He J-H, Cai X-C, Kang Y-T, Mao Y. RP-HPLC determination of related substances of hemin. Chin J Pharl Anal. 2013;33:274–7.
12. Lombardo ME, Araujo LS, Ciccarelli AB, Batlle A. A spectrophotometric method for estimating hemin in biological systems. Anal Biochem. 2005;341:199–203. https://doi.org/10.1016/j.ab.2004.11.002.
13. Takahashi S, Bhowmik S, Sugimoto N. Volumetric analysis of formation of the complex of G-quadruplex DNA with hemin using high pressure. J Inorg Biochem. 2017;166:199–207. https://doi.org/10.1016/j.jinorgbio.2016.08.011.
14. Benavides J, Quijada-Garrido I, García O. The synthesis of switch-off fluorescent water-stable copper nanocluster Hg2+ sensors via a simple one-pot approach by an in situ metal reduction strategy in the presence of a thiolated polymer ligand template. Nanoscale. 2020;12(2):944–55. https://doi.org/10.1039/C9NR08439H.
15. Feng X, Zhang J, Wang J, Han A, Fang G, Liu J, et al. The stabilization of fluorescent copper nanoclusters by dialdehyde cellulose and their use in mercury ion sensing. Anal Methods. 2020;12(24):3130–6. https://doi.org/10.1039/D0AY00657B.
16. Zhao Y, Zhou H, Zhang S, Xu J. The synthesis of metal nanoclusters and their applications in bio-sensing and imaging. Methods and Applications in Fluorescence. 2019;8(1):012001. https://doi.org/10.1088/2050-6120/ab57e7.
17. Chen Y, Dong X, Zheng Y, Wang Y, Guo Z, Jiang H, et al. A novel turn-on fluorescent sensor for the sensitive detection of glutathione via gold nanocluster preparation based on controllable ligand-induced etching. Analyst. 2020;145(12):4265–75. https://doi.org/10.1039/D0AN00807A.

18. Zhang G, Li Y, Xu J, Zhang C, Shuang S, Dong C, et al. Glutathione-protected fluorescent gold nanoclusters for sensitive and selective detection of Cu^{2+}. Sensor Actuat B: Chem. 2013;183:583–8. https://doi.org/10.1016/j.snb.2013.04.023.
19. Li Y, Wen Q-L, Liu A-Y, Long Y, Liu P, Ling J, et al. One-pot synthesis of green-emitting gold nanoclusters as a fluorescent probe for determination of 4-nitrophenol. Microchim Acta. 2020;187:106. https://doi.org/10.1007/s00604-019-4090-5.
20. Jia Y, Sun T, Jiang Y, Sun W, Zhao Y, Xin J, et al. Green, fast, and large-scale synthesis of highly fluorescent au nanoclusters for Cu^{2+} detection and temperature sensing. Analyst. 2018;143(21):5145–50. https://doi.org/10.1039/C8AN01617H.
21. Liu R, Duan S, Bao L, Wu Z, Zhou J, Yu R. Photonic crystal enhanced gold-silver nanoclusters fluorescent sensor for Hg^{2+} ion. Anal Chim Acta. 2020;1114:50–7. https://doi.org/10.1016/j.aca.2020.04.011.
22. Zhang G, Xiang M, Kong R-M, Qu F. Fluorescent and colorimetric determination of glutathione based on the inner filter effect between silica nanoparticle–gold nanocluster nanocomposites and oxidized 3,3′,5,5′-tetramethylbenzidine. Analyst. 2020;145(19):6254–61. https://doi.org/10.1039/D0AN01392G.
23. Halawa MI, Lai J, Xu G. Gold nanoclusters: synthetic strategies and recent advances in fluorescent sensing. Mater Today Nano. 2018;3:9–27. https://doi.org/10.1016/j.mtnano.2018.11.001.
24. Wang J, Lin X, Su L, Yin J, Shu T, Zhang X. Chemical etching of pH-sensitive aggregation-induced emission-active gold nanoclusters for ultra-sensitive detection of cysteine. Nanoscale. 2019;11(1):294–300. https://doi.org/10.1039/C8NR08526A.
25. Bian R-X, Wu X-T, Chai F, Li L, Zhang L-Y, Wang T-T, et al. Facile preparation of fluorescent Au nanoclusters-based test papers for recyclable detection of Hg^{2+} and Pb^{2+}. Sensor Actuat B: Chem. 2017;241:592–600. https://doi.org/10.1016/j.snb.2016.10.120.
26. Deng H-H, Deng Q, Li K-L, Zhuang Q-Q, Zhuang Y-B, Peng H-P, et al. Fluorescent gold nanocluster-based sensor for detection of alkaline phosphatase in human osteosarcoma cells. Spectrochim Acta A. 2020;229:117875. https://doi.org/10.1016/j.saa.2019.117875.
27. Yahia-Ammar A, Sierra D, Mérola F, Hildebrandt N, Le Guével X. Self-assembled gold nanoclusters for bright fluorescence imaging and enhanced drug delivery. ACS Nano. 2016;10:2591–9. https://doi.org/10.1021/acsnano.5b07596.
28. Chang H-C, Ho J-aA. Gold nanocluster-assisted fluorescent detection for hydrogen peroxide and cholesterol based on the inner filter effect of gold nanoparticles. Anal Chem. 2015;87:10362–7. https://doi.org/10.1021/acs.analchem.5b02452.
29. Alkilany A, Alsotari S, Alkawareek M, Abulateefeh S. Facile hydrophobication of glutathione-protected gold nanoclusters and encapsulation into poly(lactide-co-glycolide) nanocarriers. Sci Rep. 2019;9. https://doi.org/10.1038/s41598-019-47543-4.
30. Govindaraju S, Ankireddy SR, Viswanath B, Kim J, Yun K. Fluorescent gold nanoclusters for selective detection of dopamine in cerebrospinal fluid. Sci Rep. 2017;7:40298. https://doi.org/10.1038/srep40298.
31. Thakur NS, Mandal N, Banerjee UC. Esterase-mediated highly fluorescent gold nanoclusters and their use in ultrasensitive detection of mercury: synthetic and mechanistic aspects. ACS Omega. 2018;3(12):18553–62. https://doi.org/10.1021/acsomega.8b02505.
32. Chen Y-S, Kamat PV. Glutathione-capped gold nanoclusters as photosensitizers. Visible light-induced hydrogen generation in neutral water. J Am Chem Soc. 2014;136(16):6075–82. https://doi.org/10.1021/ja5017365.
33. Lu F, Yang H, Tang Y, Yu C-J, Wang G, Yuan Z, et al. 11-Mercaptoundecanoic acid capped gold nanoclusters with unusual aggregation-enhanced emission for selective fluorometric hydrogen sulfide determination. Microchim Acta. 2020;187(4):200. https://doi.org/10.1007/s00604-020-4159-1.
34. Zhang H, Liu Q, Wang T, Yun Z, Li G, Liu J, et al. Facile preparation of glutathione-stabilized gold nanoclusters for selective determination of chromium (III) and chromium (VI) in environmental water samples. Anal Chim Acta. 2013;770:140–6. https://doi.org/10.1016/j.aca.2013.01.042.
35. Feng B, Xing Y, Lan J, Su Z, Wang F. Synthesis of MUC1 aptamer-stabilized gold nanoclusters for cell-specific imaging. Talanta. 2020;212:120796. https://doi.org/10.1016/j.talanta.2020.120796.
36. Qian H, Zhu M, Wu Z, Jin R. Quantum sized gold nanoclusters with atomic precision. Acc Chem Res. 2012;45(9):1470–9. https://doi.org/10.1021/ar200331z.
37. Sang F, Zhang X, Shen F. Fluorescent methionine-capped gold nanoclusters for ultra-sensitive determination of copper(II) and cobalt(II), and their use in a test strip. Microchim Acta. 2019;186(6):373. https://doi.org/10.1007/s00604-019-3428-3.
38. Talavera C, Kamat PV. Glutathione-capped gold nanoclusters: photoinduced energy transfer and singlet oxygen generation. J Chem Sci. 2018;130:143. https://doi.org/10.1007/s12039-018-1549-6.
39. Gao L, Xiao Y, Wang Y, Chen X, Zhou B, Yang X. A carboxylated graphene and aptamer nanocomposite-based aptasensor for sensitive and specific detection of hemin. Talanta. 2015;132:215–21. https://doi.org/10.1016/j.talanta.2014.09.010.
40. Wu Z, Jin R. On the ligand's role in the fluorescence of gold nanoclusters. Nano Lett. 2010;10(7):2568–73. https://doi.org/10.1021/nl101225f.
41. Su X, Jiang H, Wang X. Thiols-induced rapid photoluminescent enhancement of glutathione-capped gold nanoparticles for intracellular thiols imaging applications. Anal Chem. 2015;87(20):10230–6. https://doi.org/10.1021/acs.analchem.5b02559.
42. Khataee A, Jalili R, Dastborhan M, Karimi A, Ebadi Fard Azar A. Ratiometric visual detection of tetracycline residues in milk by framework-enhanced fluorescence of gold and copper nanoclusters. Spectrochim Acta A. 2020;242:118715. https://doi.org/10.1016/j.saa.2020.118715.
43. Meng L, Wu Y, Xu N. Gold nanoclusters fluorescence probe for monitoring chloramphenicol and study of two-dimensional correlation fluorescence spectroscopy. J Mol Struc. 2021;1223:128875. https://doi.org/10.1016/j.molstruc.2020.128875.
44. Liu G, Feng D-Q, Hua D, Liu T, Qi G, Wang W. Fluorescence enhancement of terminal amine assembled on gold nanoclusters and its application to ratiometric lysine detection. Langmuir. 2017;33(51):14643–8. https://doi.org/10.1021/acs.langmuir.7b02614.
45. Soleilhac A, Bertorelle F, Comby-Zerbino C, Chirot F, Calin N, Dugourd P, et al. Size characterization of glutathione-protected gold nanoclusters in the solid, liquid and gas phases. J Phys Chem C. 2017;121:27733–40. https://doi.org/10.1021/acs.jpcc.7b09500.
46. Xu X, Ji J, Chen P, Wu J, Jin Y, Zhang L, et al. Salt-induced gold nanoparticles aggregation lights up fluorescence of DNA-silver nanoclusters to monitor dual cancer markers carcinoembryonic antigen and carbohydrate antigen 125. Anal Chim Acta. 2020;1125:41–9. https://doi.org/10.1016/j.aca.2020.05.027.
47. Wang Y, Chen T, Zhang Z, Ni Y. Cytidine-stabilized copper nanoclusters as a fluorescent probe for sensing of copper ions and hemin. RSC Adv. 2018;8(17):9057–62. https://doi.org/10.1039/C7RA11383H.
48. Jiang H, Zhang W, Li J, Nie L, Wu K, Duan H, et al. Inner-filter effect based fluorescence-quenching immunochromotographic assay for sensitive detection of aflatoxin B1 in soybean sauce. Food Control. 2018;94:71–6. https://doi.org/10.1016/j.foodcont.2018.06.030.
49. Goldstein L, Teng Z-P, Zeserson E, Patel M, Regan RF. Hemin induces an iron-dependent, oxidative injury to human neuron-like cells. J Neurosci Res. 2003;73(1):113–21. https://doi.org/10.1002/jnr.10633.

50. Gao S, Wang R, Bi Y, Qu H, Chen Y, Zheng L. Identification of frozen/thawed beef based on label-free detection of hemin (Iron Porphyrin) with solution-gated graphene transistor sensors. Sensor Actuat B: Chem. 2020;305:127167. https://doi.org/10.1016/j.snb.2019.127167.
51. Guo Z, Li B, Zhang Y, Zhao Q, Zhao J, Li L, et al. Acid-treated graphitic carbon nitride nanosheets as fluorescence probe for detection of hemin. ChemistrySelect. 2019;4(28):8178–82. https://doi.org/10.1002/slct.201901841.
52. Shi Y, Huang WT, Luo HQ, Li NB. A label-free DNA reduced graphene oxide-based fluorescent sensor for highly sensitive and selective detection of hemin. Chem Commun. 2011;47(16):4676–8. https://doi.org/10.1039/C0CC05518B.
53. Zhang Z, Hu B, Zhuang Q, Wang Y, Luo X, Xie Y, et al. Green synthesis of fluorescent nitrogen–sulfur co-doped carbon dots from scallion leaves for hemin sensing. Anal Lett. 2020;53(11):1704–18. https://doi.org/10.1080/00032719.2020.1716782.
54. Baruah U, Gogoi N, Majumdar G, Chowdhury D. Capped fluorescent carbon dots for detection of hemin: role of number of -OH groups of capping agent in fluorescence quenching. Sci World J. 2013;2013:529159. https://doi.org/10.1155/2013/529159.
55. Shekari Z, Zare HR, Falahati A. An ultrasensitive aptasensor for hemin and hemoglobin based on signal amplification via electrocatalytic oxygen reduction. Anal Biochem. 2017;518:102–9. https://doi.org/10.1016/j.ab.2016.11.016.
56. Neugebauer U, März A, Henkel T, Schmitt M, Popp J. Spectroscopic detection and quantification of heme and heme degradation products. Anal Bioanal Chem. 2012;404:2819–29. https://doi.org/10.1007/s00216-012-6288-9.